Hybrid density-functional calculations of phonons in $LaCoO_3$

Denis Gryaznov,[1,2,*] Robert A. Evarestov,[3] and Joachim Maier[1]
[1]*Max Planck Institute for Solid State Research, Heisenbergstr. 1, D-70569 Stuttgart, Germany*
[2]*Institute for Solid State Physics, Kengaraga 8, LV-1063 Riga, Latvia*
[3]*Department of Quantum Chemistry, St. Petersburg University, Universitetsky Prosp. 26, 198504 St. Petergof, Russia*
(Received 2 August 2010; revised manuscript received 26 October 2010; published 2 December 2010)

Phonon frequencies at Γ point in nonmagnetic rhombohedral phase of $LaCoO_3$ were calculated using density-functional theory with hybrid exchange correlation functional PBE0. The calculations involved a comparison of results for two types of basis functions commonly used in *ab initio* calculations, namely, the plane-wave approach and linear combination of atomic orbitals, as implemented in VASP and CRYSTAL computer codes, respectively. A good qualitative, but also within an error margin of less than 30%, a quantitative agreement was observed not only between the two formalisms but also between theoretical and experimental phonon frequency predictions. Moreover, the correlation between the phonon symmetries in cubic and rhombohedral phases is discussed in detail on the basis of group-theoretical analysis. It is concluded that the hybrid PBE0 functional is able to predict correctly the phonon properties in $LaCoO_3$.

DOI: 10.1103/PhysRevB.82.224301 PACS number(s): 63.20.dk, 71.15.Mb, 31.15.A−

I. INTRODUCTION

From the application point of view, it should be mentioned that cobaltite based electrode materials are extensively studied for oxygen permeation membranes[1] and fuel cells.[2] $LaCoO_3$ is a strongly correlated material with a Co-O covalent bonding. $LaCoO_3$ attracts great interest from researchers due to its complex magnetic behavior and interesting phase diagram. One of the key issues to be solved concerns the magnetic phase transition from the low-spin state (LS: $t_{2g}^6 e_g^0 \rightarrow a_{1g}^2 e_g^4 e_g^0$, i.e., $S=0$, here splitting of $3d$ levels of Co in cubic and rhombohedral crystal fields, respectively, is shown) to excited high-spin state (HS: $t_{2g}^4 e_g^2 \rightarrow a_{1g}^2 e_g^2 e_g^2$, i.e., $S=2$) or intermediate spin state (IS: $t_{2g}^5 e_g^1 \rightarrow a_{1g}^2 e_g^3 e_g^1$, $S=1$).[3,4] Also, the semiconductor-metal transition at ~500 K is still not properly understood.[5] As the standard density-functional-theory (DFT) exchange-correlation functionals predict $LaCoO_3$ magnetic and metallic at low temperatures opposite to experiments (see discussion below), obviously a careful theoretical treatment is required. The majority of publications discussing the *ab initio* calculation results for $LaCoO_3$ are based on the so-called LDA(GGA)+U method, which was shown to reproduce correctly a nonmagnetic behavior of $LaCoO_3$ at low temperatures.[6,7] A commonly used approach is to find the U parameter by fitting materials properties to experimental values.[8] The U values so far discussed in the literature for $LaCoO_3$ vary in the range between ~3 and ~8 eV depending on the basis and Hamiltonian. These techniques demonstrated a LS ground state and an IS state to be the lowest excited state and, thus, proposed an explanation to controversy on the magnetic phase transition appearing at temperatures close to 90 K.[6]

Recent quantum chemical nonperiodic (embedded cluster) linear combination of atomic orbitals (LCAOs) calculations did not confirm the stabilization of IS state against the HS state.[9] In these calculations the restricted Hartree-Fock method and atom-centered Gaussian-type orbitals were applied. However, the LS state was found to be stabilized only if dynamical electron correlation effects were included.

It is worth mentioning, that the magnetic phase transitions discussed are thermally induced. The temperature effects could be included by calculating the phonon frequencies as the prerequisite to free energies.

In the present study the two different periodic approaches [namely, LCAO and plane wave (PW)] are applied to calculate the phonon frequencies for the LS state of $LaCoO_3$ within the same hybrid exchange-correlation functional, namely, PBE0.[10] The results are also compared with recently published LDA+U study of Laref and Luo.[11] Unlike the LDA(GGA)+U method, the hybrid PBE0 functional does not require any adjustable parameters and has been deduced on the basis of pure theoretical grounds.[10] This functional has shown to properly reproduce the properties of many strongly correlated systems (see, for example, Ref. 12).

The calculations of $LaCoO_3$ phonon frequencies were based on the following procedure. First, the equilibrium geometry was found by optimizing the structure parameters (see discussion below) for the $D_{3d}^6(R\bar{3}c)$ space group. The rhombohedral cell parameters were compared with experimental data. Second, the phonon frequencies were obtained within the frozen phonon method[13,14] at the fixed equilibrium structure parameters.

II. COMPUTATIONAL DETAILS

The phonon frequencies in the LCAO basis were calculated in CRYSTAL09.[15] The Gaussian basis set and pseudopotentials (PPs) of free atoms for La and Co were taken from the PPs library of the Stuttgart/Cologne group.[16] The relativistic PP for La included 46 electrons and for Co ten electrons. In order to avoid spurious interactions between the diffuse functions and the core functions of neighboring atoms, the basis set diffuse exponents smaller than 0.15 (in $Bohr^{-2}$) for La and Co were removed. The all electron basis set $8-411G^*$ from Ref. 17 was used for O atom for this nonoptimized basis set (hereafter, BS1). In the optimized basis set (hereafter, BS2) the exponents of noncontracted basis functions were optimized by the method of conjugate

TABLE I. A comparison of rhombohedral lattice constant a (in Å), angle α (in °), the O position free parameter u (in fraction of the lattice constant), effective charge Q (in e^-) of La, Co, and O atoms, and band gap E_g (in eV) for different methods used in the present study and the experiment.

Method	a	α	u	Q_{Co}	Q_{La}	Q_O	E_g
LCAO PBE (BS2)	5.41	61.48	0.193	1.30	2.66	−1.32	Metal
LCAO PBE0 (BS1)	5.34	60.86	0.209	0.95	2.76	−1.24	3.19
LCAO PBE0 (BS2)	5.36	60.83	0.206	1.40	2.73	−1.38	3.14
PW PBE	5.37	61.53	0.186	1.40	2.09	−1.16	Metal
PW PBE0	5.33	61.01	0.195	1.62	2.23	−1.28	2.50
LDA+U (Ref. 11)	5.34	60.91	0.195				~1.8
Expt.	5.34[a]	60.99[a]	0.198[a]	3[b]	3[b]	−2[b]	0.6[c]

[a]At 4 K, Ref. 23.
[b]Formal charge.
[c]Reference 29.

directions[18] as implemented in the OPTBAS code.[19] The role of BS optimization is discussed by comparing phonon frequencies and bulk properties for both the BSs. The Monkhorst-Pack scheme for $8\times8\times8$ k-point mesh in the Brillouin zone was applied together with the tolerances 7, 7, 7, 7, and 14 for the Coulomb and exchange integrals calculations. The tolerances were increased to 10, 10, 10, 10, and 16 for the phonon frequency calculations. Furthermore, the forces for the self-consistent cycles were optimized until the energy difference reached 10^{-6} eV for the lattice structure optimization and 10^{-8} eV for the phonon frequency calculations.

The phonon frequencies in the PW basis were calculated in VASP code,[20,21] which represents an effective tool for solid-state calculations based on the ultrasoft pseudopotentials approach and PWs. We used the projector augmented wave method[22] and scalar-relativistic PPs substituting for 46 core electrons on La atom, 18 core electrons on Co atoms, and two core electrons on O atom. The plane wave cut-off energy was fixed at 520 eV for the geometry optimization and increased to 600 eV for the phonon frequency calculations. The tolerance for forces calculations and the Monkhorst-Pack scheme were the same as in the CRYSTAL calculations. The electron occupancies were determined with the Gaussian method using a smearing parameter of 0.1 eV.

III. RESULTS AND DISCUSSION

A. Bulk properties

$LaCoO_3$ has a rhombohedrally distorted perovskite structure known to exist within a broad temperature range.[23–25] Table I presents the results of *ab initio* PBE and PBE0 calculations for structure parameters, effective charges (due to Mulliken analysis in CRYSTAL (Ref. 26) and Bader analysis[27,28] in VASP) and the electronic band gap. The results are also compared to experimental data. It is worth mentioning that the standard DFT exchange-correlation functional (PBE) predicts $LaCoO_3$ to be metallic using the LCAO as well as PW approach. Contrary, the hybrid PBE0 functional suggests that $LaCoO_3$ is insulating with a band gap E_g of 2.5 and 3.14 eV in the PW and LCAO (BS2) calculations, respectively. Such values of E_g are higher than those known from the LDA(GGA)+U calculations: 1.0,[7] 1.43,[8] and 2.0 eV.[6] It can, at least partly, be explained by the exact exchange part of the PBE0 functional which tends to overestimate E_g. The ultraviolet photoemission spectroscopy if combined with the bremsstrahlung isochromat spectroscopy[29] can provide us with the measured value of E_g. However, the value of E_g suggested in Ref. 29 is smaller than our value found using the hybrid functionals (Table I). The interpretation of measured spectra is not simple and Saitoh *et al.*[30] also deduced the value of 2 eV from Ref. 29. Moreover, the value for E_g obtained in the LDA+U (Ref. 11) or GGA+U (as well as LSDA+U) (Ref. 31) study at $U\sim8$ eV is close to 1.5 eV. Note that E_g is very sensitive to the U parameter.[31] It is obvious that $LaCoO_3$ is a nonmagnetic insulator at low temperatures which is correctly reproduced within our *ab initio* calculations. The total energy difference between the LS and IS states is ~−0.1 eV per primitive unit cell whereas the same between the LS and HS is ~−1.5 eV per primitive unit cell in the LCAO calculations with the PBE0 functional. The lattice parameters are very well reproducible using the PBE0 functional (the errors of the order 1% or less). The standard PBE functional slightly overestimates the rhombohedral lattice constant a and angle α. The coordinates of O atoms in the D_{3d}^6 space group are characterized by the free parameter u (see also Table II). The value of u is underestimated by the PBE functional. This is why; the PBE functional was excluded from our following analysis of calculated phonon frequencies. There is, however, a very good agreement on the parameter u between the LDA+U study[11] and present PBE0 calculations in the PW basis. In contrast, the LCAO calculations suggest slightly higher values of u.

In Fig. 1 a comparison of density of states calculated for the rhombohedral phase of $LaCoO_3$ is shown for the PBE0 functional in two codes used in the present study. Both the codes agree on the fact that the valence band represents strong hybridization of electrons of O and Co atoms with some small contribution from La. The same effect was found in the GGA+U study[31] with U=3.4 eV. The valence band is characterized by two peaks at ~−4.5(−4.3) and ~−1.0(−0.5) eV below the Fermi energy in the PW (LCAO) calculations being, thus, in good agreement with the

TABLE II. Atomic Wyckoff position, site symmetry, and simple induced representations (irreps) of the O_h^1 and D_{3d}^6 space groups.

$O_h^1(Pm\bar{3}m)$			$D_{3d}^6(R\bar{3}c)$	
	irreps			irreps
Wyckoff position	Γ	R	Wyckoff position	Γ
La-$a(0,0,0)$ O_h, $t_{1u}(x,y,z)$	$4^-(t_{1u})$	4^-	La-$2a(\frac{1}{4},\frac{1}{4},\frac{1}{4})$ C_{3v}, $a_2(z)$ $e(x,y)$	$2^+(a_{2g})\ 2^-(a_{2u})$ $3^+(e_g)\ 3^-(e_u)$
Co-$b(\frac{1}{2},\frac{1}{2},\frac{1}{2})$ O_h, $t_{1u}(x,y,z)$	$4^-\ (t_{1u})$	5^+	Co-$2b(0,0,0)$ C_{3i}, $a_u(z)$ $e_u(x,y)$	$1^-(a_{1u})\ 2^-(a_{2u})$ $2\times 3^-(e_u)$
O-$d(0,0,\frac{1}{2})$ D_{4h}, $a_{2u}(z)$ $e_u(x,y)$	$4^-\ (t_{1u})$ $4^-\ (t_{1u})\ 5^-\ (t_{2u})$	1^+3^+ 4^+5^+	O-$6e(-u,u+\frac{1}{2},\frac{3}{4})$ C_2, $a(z)$ $2b(x,y)$	$1^+(a_{1g})\ 1^-(a_{1u})\ 3^+(e_g)\ 3^-(e_u)$ $2\times 2^+(a_{2g})\ 2\times 2^-(a_{2u})\ 2\times 3^+(e_g)\ 2\times 3^-(e_u)$

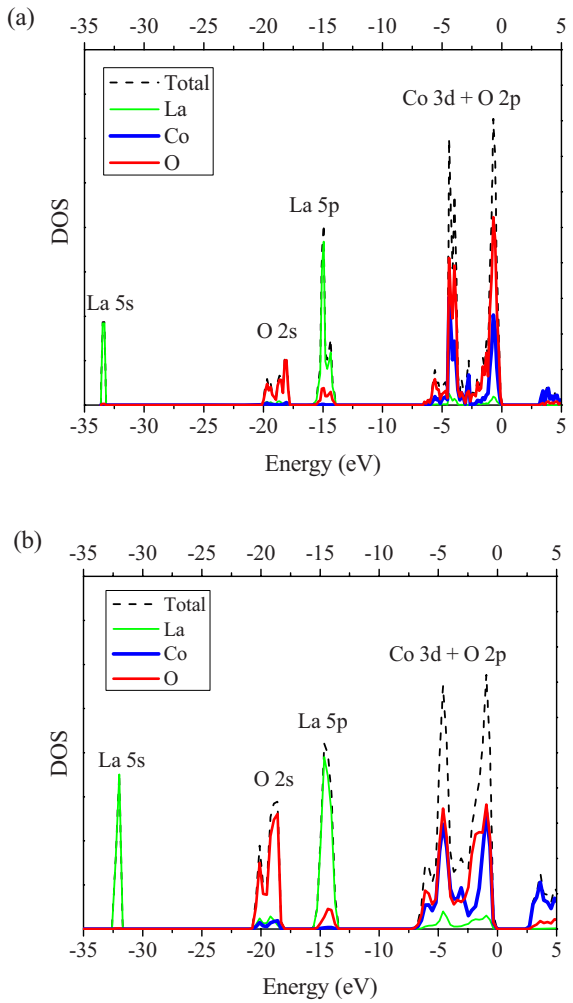

FIG. 1. (Color online) The total and partial density of states for rhombohedral phase of $LaCoO_3$ using the hybrid PBE0 functional in (a) CRYSTAL and (b) VASP codes. The Fermi energy is taken as 0.

experiments.[29] Moreover, the position of La 5p band is also approximately the same in both the codes. Only the O 2s (La 5s) band is slightly shifted by ~1.0(−1.5) eV in CRYSTAL in comparison to VASP. In contrast, the GGA+U study[31] suggests strong hybridization between different electrons in comparison to our PBE0 study. For example, the position of La 5p band differs by almost 10 eV between the GGA+U study and our results. The overall picture suggests a very good agreement between the PBE0 functionals in the PW and LCAO codes.

B. Phonon symmetry

Table II gives the symmetry of phonons in two $LaCoO_3$ structures: the cubic O_h^1 and rhombohedral D_{3d}^6. The symmetry is defined by the corresponding space group irreducbile representations (irreps) induced from atom site symmetry group irreps corresponding to the atomic displacement x,y,z. In particular, the O atom in the d position in the cubic structure has D_{4h} symmetry. However, its local symmetry in D_{3d}^6 is reduced to C_2 and coordinates are determined by free parameter u which defines the rhombohedral angle. One can see that the O and Co atoms contribute to the a_{1u} irrep, the O and La atoms to the a_{2g} and e_g irreps, all three atoms—to the a_{2u} and e_u irreps, and there is one a_{1g} irrep determined by the O atom only. Table II also shows that the t_{1u} irrep of La in the cubic crystal is splitted into a_{2u} and e_u in the rhombohedral crystal whereas the a_{2g} and e_g are appearing by the projection of R point of the cubic crystal onto Γ point in the rhombohedral crystal. On the other hand, the t_{1u} irrep of Co in the cubic crystal is splitted into a_{1u} and e_u in the rhombohedral crystal, and R_5^+ in the cubic crystal is splitted into a_{1u} and e_u in the rhombohedral crystal. Further aspects on the symmetry correlations between different phases of perovskitelike materials can be found in Ref. 32. These are important to include for the structure phase transitions and crystal-field effects analysis.

TABLE III. Phonon symmetry (only active modes) and frequencies ν_{th} in cm^{-1} calculated in VASP (PW) and CRYSTAL (LCAO) with the PBE0 exchange-correlation functional. The experimental Raman and IR frequencies ν_{exp} from Refs. 33–35, respectively, and the phonon modes from the LDA+U study are also given. The values in the parenthesis represent the relative errors with respect to the experimental values in %.

Phonon symmetry	Raman active					Acoustic		IR active							
	e_g	e_g	a_{1g}	e_g	e_g	e_u	a_{2u}	a_{2u}	e_u	e_u	a_{2u}	e_u	e_u	a_{2u}	e_u
ν_{exp}	86	172	261	432	584	0	0	177,[a] 180,[b]	174+240 [b]	242[a]	315,[a] 330,[b]	328+411 [b]	411[a]	540,[a] 600,[b]	550+582 [b]
LCAO, PBE0, (BS1)	108, (26)	193, (12)	238, (9)	452, (5)	646, (11)	5.1i	0.1i	196, (13)	209, (13)	280, (16)	327, (0)	364, (11)	433, (5)	554, (1)	565, (3)
LCAO, PBE0, (BS2)	104, (21)	178, (3)	257, (1)	448, (3)	631, (8)	0.7i	0.0	171, (2)	193, (20)	273, (13)	329, (0)	362, (12)	433, (5)	536, (2)	551, (5)
PW, PBE0	57, (34)	178, (3)	280, (7)	438, (1)	613, (5)	4i	5i	151, (13)	177, (26)	247, (2)	305, (7)	351, (15)	441, (7)	513, (7)	532, (9)
PW, LDA+U [c]	78, (9)	174, (1)	253, (3)	409, (5)	448, (23)			72, (59)	53, (78)	79, (67)	532, (62)	111, (73)	158, (62)	652, (18)	412, (29)

[a]Reference 34.
[b]Reference 35.
[c]Reference 11.

C. Calculated phonon frequencies

A crystal with rhombohedral structure such as $LaCoO_3$ has the following set of optical phonon modes at Γ point: $a_{1g}+4e_g+6e_u+4a_{2u}+3a_{2g}+2a_{1u}$ (Table II). All such calculated modes except for $3a_{2g}$ and $2a_{1u}$ are given in Table III for the PBE0 functional in two codes together with the experimental frequencies ν_{exp} from the literature. The latter two modes are silent and are not visible in optical experiments. Owing to errors in the numerical calculation of total energy second derivative over the displacements, two acoustic modes are not exactly zero but small imaginary numbers. In Table III the relative errors with respect to ν_{exp} are defined as $|\nu_{exp}-\nu_{th}|/\nu_{exp}100\%$, where ν_{th} is the calculated frequency. The Raman active phonon modes calculated in both CRYSTAL and VASP are close to ν_{exp} from Ref. 32. The LCAO basis optimization (BS2 vs BS1) improves the Raman active ν_{th}, suggesting the largest error of 21% for the lowest e_g frequency with respect to the experiment. The PW PBE0 calculations show an error of 34% for the same mode. Additionally, the results from the LDA+U study[11] are given in Table III. The lowest e_g frequency is better reproduced in their study whereas the highest e_g frequency is obtained with the error 23% opposite to 5% in our PBE0 calculations. In order to properly discuss the IR modes; one has to keep in mind, that the eight IR active optical modes in the rhombohedral crystal are splitted into $3(a_{2u}+e_u)$ combinations and $2e_u$ modes. The three pairs are denoted in the literature as external, bending and stretching modes from low to high frequencies. The experimental phonon modes from the reflectivity spectra of Yamaguchi *et al.*[34] and Tajima *et al.*[35] showed three major peaks. The low-temperature measurements of Yamaguchi *et al.* could also identify weak peaks from the two e_u modes whereas Tajima *et al.* suggested partial assignment of the $3(a_{2u}+e_u)$ peaks: the peaks were separated into pairs, however, a complete assignment of a_{2u} and e_u is not clear. On the basis of the fact that the a_{2u} mode in all the calculations has lower frequency, we divided six frequencies from Table I in Ref. 35 into a_{2u} and e_u modes and compared them to the calculated frequencies. For the $3(a_{2u}+e_u)$ pairs the a_{2u} mode is well comparable to the experiment with the maximum error 13% for the BS1 basis in LCAO PBE0 calculations. The basis optimization reduced this error to 2% only (see BS2 in Table III). Contrary, the e_u modes are worse comparable to the experiment (the maximum error 20% for the lowest e_u frequency). Similar results were also observed for the PW PBE0 calculations: the error 26% for the lowest e_u mode. Such high errors for the e_u modes may be also related to limitations of the experiment in Ref. 35 due to only partial symmetry assignment. The other two weak e_u modes are perfectly reproduced in the PW PBE0 calculation (errors of 2% and 7%, respectively) and a bit worse in the LCAO PBE0 calculation for BS2 (errors 13% and 5%). However, the IR frequencies are poorly reproduced in the LDA+U calculation[11] leading to errors as high as 60% for majority modes.

IV. CONCLUSIONS

Several DFT approaches available to calculate the phonon frequencies were compared for $LaCoO_3$. We have clearly shown that the PBE0 exchange-correlation functional is able to predict the phonon frequencies in $LaCoO_3$, independently of the basis choice (LCAO and PW). Also, we have observed a trend that the highest errors in the phonon frequencies calculated by the frozen phonon method appear for the lowest frequencies; the errors decrease for the intermediate frequencies, and slightly increase for the highest frequencies. We believe that this is a general trend, which must be taken in the analysis of calculated phonon frequencies. The results as obtained in the present study are very important for future analysis of spin state transitions using phonon modes and calculating thermodynamic properties in $LaCoO_3$.

ACKNOWLEDGMENTS

This study was partly supported by EC NASA—OTM project. The authors are grateful to Manuel Cardona, Natalya Kovaleva, and Eugene Kotomin for helpful discussions, and Maxim Losev for the support with the OPTBAS package.

*d.gryaznov@fkf.mpg.de

[1] Z. Shao, W. Yang, Y. Cong, H. Dong, J. Tong, and G. Xiong, J. Membr. Sci. **172**, 177 (2000).
[2] C. Sun, R. Hui, and J. Roller, J. Solid State Electrochem. **14**, 1125 (2010).
[3] J. B. Goodenough, J. Phys. Chem. Solids **6**, 287 (1958); P. M. Raccah and J. B. Goodenough, Phys. Rev. **155**, 932 (1967).
[4] J.-Q. Yan, J.-S. Zhou, and J. B. Goodenough, Phys. Rev. B **69**, 134409 (2004).
[5] Y. Tokura, Y. Okimoto, S. Yamaguchi, H. Taniguchi, T. Kimura, and H. Takagi, Phys. Rev. B **58**, R1699 (1998).
[6] M. A. Korotin, S. Yu. Ezhov, I. V. Solovyev, V. I. Anisimov, D. I. Khomskii, and G. A. Sawatzky, Phys. Rev. B **54**, 5309 (1996).
[7] K. Knížek, Z. Jirák, J. Hejtmánek, P. Novák, and W. Ku, Phys. Rev. B **79**, 014430 (2009).
[8] H. Hsu, K. Umemoto, M. Cococcioni, and R. Wentzcovitch, Phys. Rev. B **79**, 125124 (2009).
[9] L. Siurakshina, B. Paulus, V. Yushankhai, and E. Sivachenko, Eur. Phys. J. B **74**, 53 (2010).
[10] J. P. Perdew, M. Ernzerhof, and K. Burke, J. Chem. Phys. **105**, 9982 (1996).
[11] A. Laref and S.-J. Luo, J. Phys. Soc. Jpn. **79**, 064702 (2010).
[12] I. D. Prodan, G. E. Scuseria, and R. L. Martin, Phys. Rev. B **76**, 033101 (2007).
[13] R. A. Evarestov and M. V. Losev, J. Comput. Chem. **30**, 2645 (2009).
[14] K. Parlinski, Z.-Q. Li, and Y. Kawazoe, Phys. Rev. Lett. **78**, 4063 (1997).
[15] R. Dovesi, V. R. Saunders, C. Roetti, R. Orlando, C. M. Zocovich-Wilson, F. Pascale, B. Civalleri, K. Doll, N. M. Harrison, I. J. Bush, Ph. D'Arco, and M. Llunell, *CRYSTAL-09 User's Manual* (University of Turin, Turin, 2010).
[16] Available online at: http://www.theochem.uni-stuttgart.de/pseudopotentials/clickpse.html
[17] T. Bredow, K. Jug, and R. A. Evarestov, Phys. Status Solidi B **243**, R10 (2006).
[18] W. H. Press, S. A. Teukolski, V. T. Vetterling, and B. P. Flannery, *Numerical Recipes in FORTRAN 77: The Art of Scientific Computing* (Press Sindicate of the University of Cambridge, NY, USA, 2001), Vol. 1.
[19] R. A. Evarestov, A. I. Panin, A. V. Bandura, and M. V. Losev, J. Phys.: Conf. Ser. **117**, 012015 (2008).
[20] G. Kresse and J. Furthmüller, *VASP the Guide* (University of Vienna, Vienna, 2009).
[21] G. Kresse and J. Furthmüller, Comput. Mater. Sci. **6**, 15 (1996).
[22] G. Kresse and D. Joubert, Phys. Rev. B **59**, 1758 (1999).
[23] G. Thornton, B. C. Tofield, and A. W. Hewat, J. Solid State Chem. **61**, 301 (1986).
[24] Y. Kobayashi, T. Mitsunaga, G. Fujinawa, T. Arii, M. Suetake, K. Asai, and J. Harada, J. Phys. Soc. Jpn. **69**, 3468 (2000).
[25] O. Haas, R. P. W. J. Struis, and J. M. McBreen, J. Solid State Chem. **177**, 1000 (2004).
[26] R. A. Evarestov, *Quantum Chemistry of Solids* (Springer, Heidelberg, 2007).
[27] R. Bader, *Atoms in Molecules: A Quantum Theory* (Oxford University Press, New York, 1990).
[28] G. Henkelman, A. Arnaldsson, and H. Jonsson, Comput. Mater. Sci. **36**, 354 (2006).
[29] A. Chainani, M. Mathew, and D. D. Sarma, Phys. Rev. B **46**, 9976 (1992).
[30] T. Saitoh, T. Mizokawa, A. Fujimori, M. Abbate, Y. Takeda, and M. Takano, Phys. Rev. B **55**, 4257 (1997).
[31] C.-L. Ma and J. Cang, Solid State Commun. **150**, 1983 (2010).
[32] R. Evarestov, arXiv:1010.1170 (unpublished).
[33] A. Ishikawa, J. Nohara, and S. Sugai, Phys. Rev. Lett. **93**, 136401 (2004).
[34] S. Yamaguchi, Y. Okimoto, and Y. Tokura, Phys. Rev. B **55**, R8666 (1997).
[35] S. Tajima, A. Masaki, S. Uchida, T. Matsuura, K. Fueki, and S. Sugai, J. Phys. C **20**, 3469 (1987).